

Supporting Information

Unlocking the effect of Cu doping in heavy metal-free AgIn₅S₈ quantum dots for highly efficient photoelectrochemical solar energy conversion

Heng Guo ^a, Jiabin Liu ^c, Bing Luo ^d, Xu Huang ^e, Jian Yang ^f, Haiyuan Chen ^b, Li Shi ^c, Xin Liu ^c, Daniele Benetti ^c, Ying Zhou ^a, Gurpreet Singh Selopal ^{*c,g}, Federico Rosei ^{*c,g}, Zhiming Wang ^{*g}, Xiaobin Niu ^{*b}

^aSchool of New Energy and Materials, Southwest Petroleum University, Chengdu, 610500, China

^bSchool of Materials and Energy, University of Electronic Science and Technology of China, Chengdu, 610054, China

^cCentre Énergie Matériaux et Télécommunications Institut National de la Recherche Scientifique 1650 Boul. Lionel Boulet, Varennes, QC J3X 1S2, Canada

^dSchool of Chemical Engineering and Technology, Xi'an Jiaotong University, Xi'an, 710049, China

^eSchool of Materials Science and Engineering, Southwest University of Science and Technology, Mianyang, 621010, China

^fKey Laboratory of Advanced Technologies of Materials (Ministry of Education), School of Materials Science and Engineering, Southwest Jiaotong University, Chengdu, 610031, China

^gInstitute of Fundamental and Frontier Science, University of Electronic Science and Technology of China, Chengdu, 610054, China

*Corresponding authors: *Email addresses*: gurpreet.selopal@emt.inrs.ca (G. S. Selopal), rosei@emt.inrs.ca (F. Rosei), zhmwang@uestc.edu.cn (Z. Wang), xbniu@uestc.edu.cn (X. Niu).

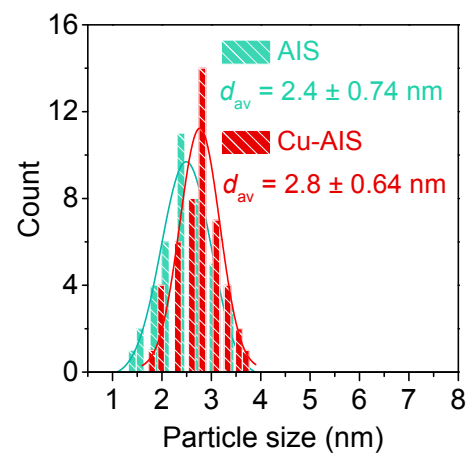


Figure S1 The size distributions of AIS and Cu-AIS QDs (the Cu doping content is 10%).

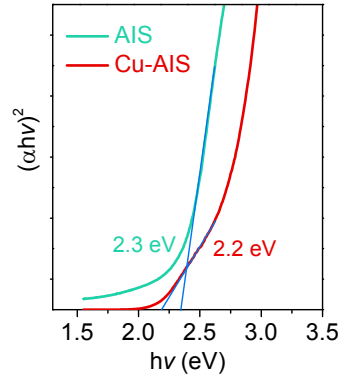


Figure S2 Tauc plot for evaluation of direct optical bandgap of AIS and Cu-AIS QDs.

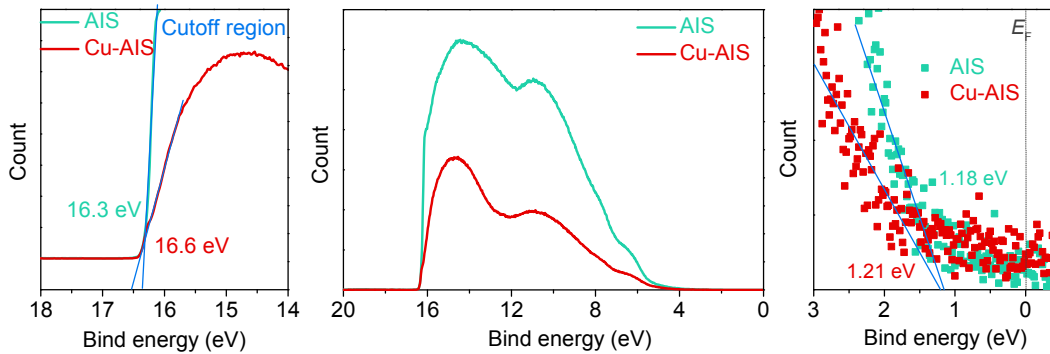


Figure S3 UPS spectra of AIS and Cu-AIS QDs. UPS full spectrum of the QDs deposited on mesoporous TiO_2 (middle), the corresponding high-resolution UPS spectrum of high binding energy cut-off (right), and low binding energy cut-off (left). According to the classical Tauc method¹, the optical band gap (E_g) values of pristine AIS and Cu-doped AISs are 2.3 eV and 2.2 eV by measuring UV-vis absorption spectra. As depicted in the secondary electron cutoff of ultraviolet photoelectron spectroscopy (UPS) used to estimate the Fermi level and maximum valence band energy level, the Fermi level of AIS and Cu-AIS QDs are -4.92 eV and -4.62 eV with respect to the vacuum level, respectively. The high binding energy cut-off (right) display that the valence band (E_{VB}) of AIS and Cu-AIS QDs are -6.10 eV and -5.83 eV with respect to the vacuum level, respectively. It is clear that the conduction band (E_{CB}) of AIS and Cu-AIS QDs are -3.80 eV and -3.63 eV with respect to the vacuum level, as obtained from $E_{CB} = E_{VB} - E_g$.

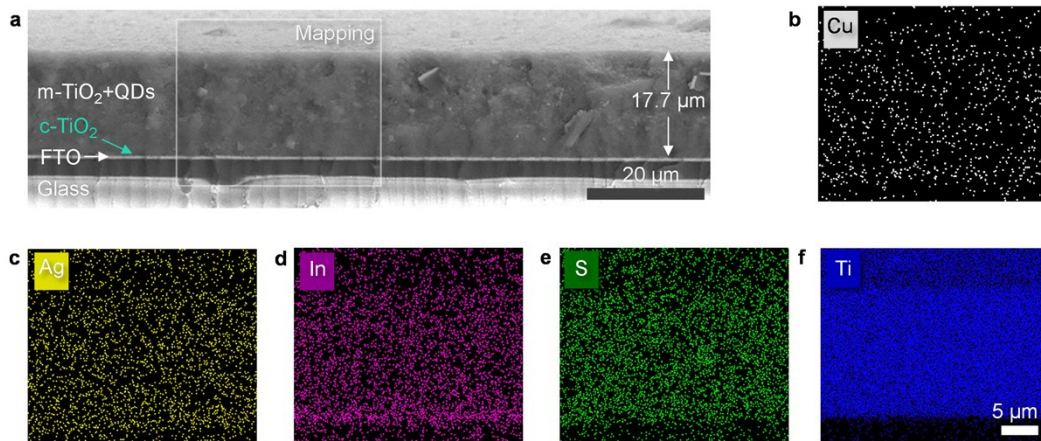


Figure S4. a) Cross-sectional SEM image of the completed Cu-AIS QDs-TiO₂ photoanode structure with relevant EDS mapping. The corresponding EDS 2D mapping of the chemical composition including the essential elements: b) Cu, c) Ag, d) In, e) S and f) Ti, respectively.

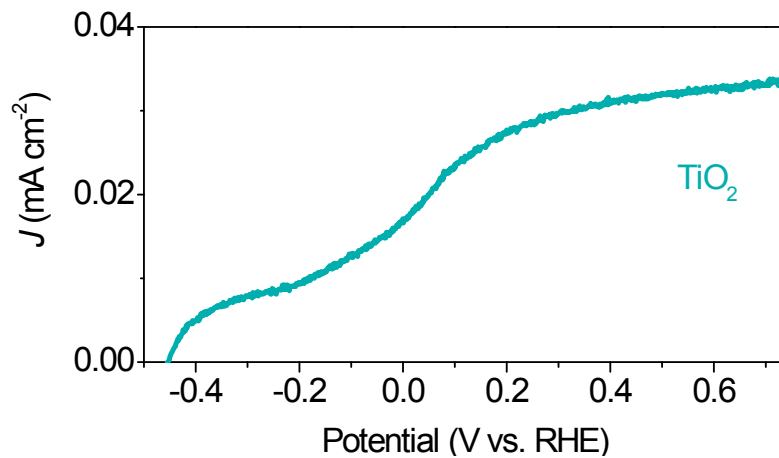


Figure S5 Photocurrent measurement with linear sweep voltammetry for the Glass|FTO|c-TiO₂|m-TiO₂ QDs sensitized photoanode photoelectrochemical cell under AM 1.5 G illumination at 100 mW cm⁻².

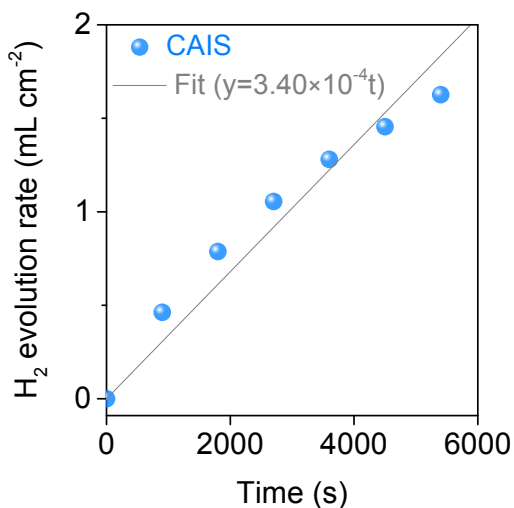


Figure S6. H₂ evolution rate of Cu-AIS QDs-based photoanode as a function of time at 0.5 V vs. RHE under AM 1.5 G illumination (100 mW cm⁻²). H₂ evolution calculation was based on the obtained photocurrent density.

The mole of H₂ was calculated according to Faraday's laws of electrolysis using the measured current based on the following formula^{2, 3}:

$$n_{H_2} = \frac{1}{z} \frac{q}{F} = \frac{1}{2} \frac{\int_{t_1}^{t_2} I dt}{F} = \frac{1}{2} \frac{I \times t}{F}$$

Where z is the number of transferred electrons per mole of water (i.e. $z = 2$). q is the quantity of electric charge in coulomb (C) and equals to $I \times t$. I is the photocurrent in amperes (A) and t is time in seconds (s). When the current is not constant, the quantity of charge passed through the circuit equals to the integration of the measured current over time (t). F is the Faraday constant (i.e. 96484.34 C/mole, $q = nF$) carried by one mole of electrons. n is the number of equivalent and equals to the numbers of H₂ moles. The above-mentioned equation is used to monitor H₂ evolution as a function of time as Cu-AIS QDs-based photoanode, exhibiting very accurate trend between photocurrent density and time. Based on the calibration curve, the evolution rate of H₂ exhibited a nearly linear increase over time. Integrated the photocurrent density in Figure 4e, the calculated hydrogen generation rate was $\approx 46.1 \mu\text{mol cm}^{-2} \text{ h}^{-1}$.

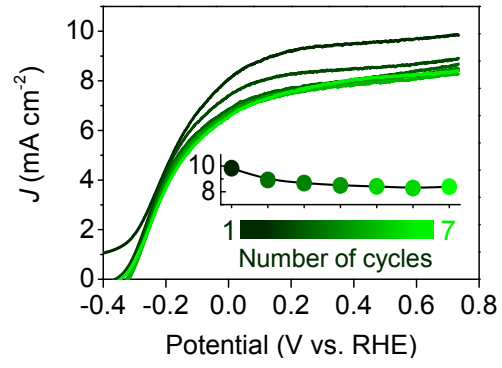


Figure S7. Photocurrent density-applied voltage (vs. RHE) versus number of cycles for the Cu-AIS QDs photoelectrochemical cell under AM 1.5 G illumination.

Table S1 Inductively coupled plasma-atomic emission spectrometry of AIS and Cu-AIS QDs. The wavelength position of the element: Cu (324.754 nm), Ag (324.068 nm), In (230.606 nm) and S (180.669 nm), respectively.

Formula ^a	Cu doping content (%)	Cu (ppm)	Ag (ppm)	In (ppm)	S (ppm)	Formula ^b
AgIn ₅ S ₈	0	0	15.97	85.49	39.52	AgIn _{5.0} S _{8.3}
Cu _{0.10} Ag _{0.90} In ₅ S ₈	10	0.69	9.02	52.49	23.96	Cu _{0.11} Ag _{0.90} In _{4.9} S _{8.0}
Cu _{0.20} Ag _{0.80} In ₅ S ₈	20	1.19	8.18	53.06	24.52	Cu _{0.19} Ag _{0.80} In _{4.9} S _{8.1}

^aCalculated by the ratio of [Cu]/[Ag] precursor used. ^bCalculated by ICP-OES analysis results.

Table S2 Fitted parameters of TRPL decay curves in AIS and Cu-AIS QDs with different Cu doping contents.

Cu doping content (%)	Absorption edge (nm)	PL peak Position (nm)	A_1	τ_1 (ns)	A_2	τ_2 (ns)	τ_{av} (ns)
0	532	677	0.0252	25.14	0.9748	242.92	242.3
5	581	723	0.0084	21.55	0.9915	351.00	350.8
10	599	730	0.0022	11.95	0.9978	375.46	375.4
15	605	735	0.0099	31.63	0.9901	338.57	338.3
20	606	738	0.0134	30.01	0.9866	298.10	297.7

Table S3 Electron transfer rate and hole transfer rate calculated from the fitted parameters of TRPL decay curves in AIS and Cu-AIS QDs with different substrates.

QDs	Substrates	A_1	τ_1 (ns)	A_2	τ_2 (ns)	τ_{av} (ns)	K_{et} ($\times 10^6 \text{ s}^{-1}$)	K_{ht} ($\times 10^6 \text{ s}^{-1}$)
	TiO ₂	0.0658	19.04	0.9342	158.40	157.23	0.80	
AIS	ZrO ₂	0.0559	21.78	0.9441	180.92	179.84		
	ZrO ₂ /Elec	0.1041	15.74	0.8959	161.98	160.35		0.68
	TiO ₂	0.2439	7.79	0.7561	66.36	64.22	9.28	
Cu-AIS	ZrO ₂	0.0616	18.86	0.9384	160.10	159.06		
	ZrO ₂ /Elec	0.1637	8.75	0.8363	85.47	83.96		5.62

References

1. W. Zhang, D. Li, M. Sun, Y. Shao, Z. Chen, G. Xiao and X. Fu, *J. Solid State Chem.*, 2010, **183**, 2466-2474.
2. B. AlOtaibi, H.P. Nguyen, S. Zhao, M.G. Kibria, S. Fan and Z. Mi, *Nano Lett.*, 2013, **13**, 4356-4361.
3. Y. Zhou, M. Celikin, A. Camellini, G. Sirigu, X. Tong, L. Jin, K. Basu, X. Tong, D. Barba, D. Ma, S. Sun, F. Vidal, M. Zavelani-Rossi, Z.M. Wang, H. Zhao, A. Vomiero and F. Rosei, *Adv. Energy Mater.*, 2017, **7**, 1602728.